UCSF
UC San Francisco Previously Published Works

Title

Neonatal development of the stratum corneum pH gradient: localization and mechanisms leading to emergence of optimal barrier function.

Permalink

https://escholarship.org/uc/item/7dm620wj

Journal

The Journal of investigative dermatology, 120(6)

ISSN

0022-202X

Authors

Behne, Martin J
Barry, Nicholas P
Hanson, Kerry M
et al.

Publication Date

2003-06-01

DOI

10.1046/j.1523-1747.2003.12262.x

License

https://creativecommons.org/licenses/by/4.0/ 4.0

Peer reviewed

eScholarship.org Powered by the California Digital Library
University of California

Neonatal Development of the Stratum Corneum pH Gradient: Localization and Mechanisms Leading to Emergence of Optimal Barrier Function

Martin J. Behne, Nicholas P. Barry*, Kerry M. Hanson*, Ida Aronchik, Robert W Clegg*, Enrico Gratton*, Kenneth Feingold, Walter M. Holleran, Peter M. Elias and Theodora M. Mauro

Although basal permeability barrier function is established at birth, the higher risk for infections, dermatitis, and percutaneous absorption of toxic agents may indicate incomplete permeability barrier maturation in the early neonatal period. Since stratum corneum (SC) acidification in adults is required for normal permeability barrier homeostasis, and lipid processing occurs via acidic pH dependent enzymes, we hypothesized that, in parallel with the less acidic surface pH, newborn SC would exhibit signs of incomplete barrier formation. Fluorescence lifetime imaging reveals that neonatal rat SC acidification first becomes evident by postnatal day 3, in extracellular "microdomains" at the SC- stratum granulosum (SG) interface, where pH-sensitive lipid processing is known to occur. This localized acidification correlated temporally with efficient processing of secreted lamellar body contents to mature extracellular lamellar bilayers. Since expression of the key acidifying mechanism NHE1 is maximal just prior to birth, and gradually declines over the first postnatal week, subop-timal SC acidification at birth cannot be attributed to insufficient NHE1 expression, but could instead reflect reduced NHE1 activity. Expression of the key lipid processing enzyme, β-glucocerebrosidase (β-GlcCer'ase), develops similar to NHE1, excluding a lack of β-GlcCer'ase protein as rate limiting for efficient lipid processing. These results define a postnatal development consisting of initial acidification in the lower SC followed by outward progression, which is accompanied by formation of mature extracellular lamellar membranes. Thus, full barrier competence appears to require the extension of acidification in microdomains from the SC/SG interface outward toward the skin surface in the immediate postnatal period.
Keywords: neonatal rat/stratum corneum pH/NHEl/FLIM/barrier function. J Invest Dermatol 120:998–1006, 2003

Full-term mammalian infants are born with a neutral skin surface pH, which normalizes to acidic values over the first few postnatal days-to-weeks, depending on species. The neutral skin surface pH of human infants was first noted by Taddei (1935), and Behrendt and Green detailed the kinetics of development of an acidic surface pH over the first postnatal month (1958). Since the skin surface pH of both full-term and premature infants acidifies rapidly during the first week (Fox *et al*, 1998; Visscher *et al*, 2001), the progressive postnatal adaptation of SC pH to ex-utcro conditions occurs independent of fetal age at birth.

In adults and neonates, formation and maintenance of the cutaneous permeability barrier requires hydrolytic processing of the relatively polar, secreted lipid mixture of lamellar bodies into their less polar lipid products, a process that is controlled by SC pH (Mauro *et al*, 1998). Two of the ''lysosomal-type'' enzymes that are required for this lipid processing, β-glucocerebrosidase (β-GlcCer'-ase) and acidic sphingomyelinase (aSM'ase), are cosecrcted with the lipids to the extracellular domains of the lower SC, but both require an acidic milieu for optimal activity (Holleran *et al*, 1992; Jensen *et al*, 1999). Despite normal basal barrier function at birth (Cunico *et al*, 1977), even full-term infants' skin exhibits a greater tendency to develop irritant/allergic contact dermatitis when exposed to alkaline or neutral solutions (Wilhelm and Maibach, 1990; Berg *et al*, 1994; Seidenari and Giusti, 1995), suggesting that barrier function is not fully mature at birth. During the immediate postnatal period, infant SC simultaneously acidifies, and reduces its susceptibility to irritants, microbes, and xe-nobiotic penetration (Harpin and Rutter, 1983; Visscher *et al*, 2000). Together, these observations suggest that development of a fully—mature perme-ability barrier is linked to SC acidification. We hypothesized, therefore, that the neutral pH of infants' skin could delay the formation of mature lipid bilayers leading to optimal barrier function, and that delayed acidification could explain the increased infantile risk for irritant/allergic contact dermatitis, infection, and percutaneous absorption of toxic chemicals.

Rats have served as a useful model to examine a range of para-meters of the peri- and neonatal adaptation process (Aszterbaum *et al*, 1992; Hoath *et al*, 1993; Wickett *et al*, 1993; Hanley *et al*, 1997). These studies have shown that the epidermal permeability barrier develops late in gestation, paralleled by increased expres-sion of pH-dependent, lipid-processing enzymes. Yet, the pH of the SC of neonatal rats is neutral, as in humans. Although the rodent model exhibits certain differences from the human neonate, notably

*Department of Dermatology, University of California San Francisco, and Dermatology Service, Veterans Affairs Medical Center, San Francisco, California, USA and *Laboratory for Fluorescence Dynamics, Department of Physics, University of Illinois, Urbana-Champaign, Illinois, USA*

Address correspondence and reprint requests to: Martin J. Behne, M.D., Veterans Affairs Medical Center, Dermatology Service (190), 4150 Clement Street, San Francisco, CA 94121, USA; bchnemj@itsa.ucsf.edu

Abbreviations: β-GlcCer'ase, β-glucocerebrosidase; CHK, cultured human kcratinocytes from foreskin; FFA, free fatty acids; FLIM, fluorescence lifetime imaging microscopy; H&E, hematoxylin-eosin; NHE1, sodium/ hydrogen antiporter 1; aSM'ase, sphingomyelinase; PL, phospholipids; SC, stratum corneum; SEM, standard error of the mean; SG, stratum granulosum; $sPLA_2$, secretory phospholipase A_2

Received 29 January 2003; revised 12 March 2003; accepted 18 March 2003

0022-202X/03/$15.00 · Copyright © 2003 by The Society for Investigative Dermatology, Inc.

the hyperplasticity of neonatal rat epidermis, and the persistence of a periderm for several days post birth (Hoath *et al*, 1993) versus the presence of vernix cascosa at birth in full-term humans (Pickens *et al*, 2000), development of the SC acid mantle occurs postnatally in both species. We therefore used newborn rats to study the adaptation of neonatal skin from the neutral pH, aqueous in-utero environment, to the dry postnatal environment. Specifically, we examined here the spatio-temporal development and changes in SC microdomain distribution of acidity during early postnatal development. Employing our newly developed application, fluorescence lifetime imaging (FLIM) (Hanson *et al*, 2002), we first localized the events leading to an acidic SC, and then correlated these changes with parallel, acidity-requiring, lipid processing in the SC interstices that produces a fully competent epidermal permeability barrier. In addition, we assessed the role of the periderm and its dissolution as a possible contributor to neonatal SC acidification.

METHODS

Materials

Pregnant sprague-dawley rats were obtained from Charles River Laboratories (Hollister, CA) and fed Purina mouse diet and water ad libitum. Newborn pups were removed individually from the litter, in approximately 24 h intervals following birth. Fetal tissue samples were generated by cesarean section, as described earlier (Aszterbaum *et al*, 1992). 2′,7′-bis(carboxyethyl)-5,6-carboxyfluorescein (BCECF) was from molecular probes (Eugene, OR). All other chemicals were of analytical grade. All experiments were performed under animal protocols reviewed and approved by the Institutional Animal Care and Use Committee (IACUC) at the VA Medical Center, San Francisco, CA.

Fluorescence lifetime imaging microscopy

pH was determined using the lifetime-sensitive fluorescent pH indicator BCECF (Molecular Probes, 100 mM applied in pure ethanol), as reported previously (Behne *et al*, 2002; Hanson *et al*, 2002). Pups were kept in a 37 °C environment and ambient humidity for the duration of the dye incubation. A biopsy was taken approximately 15 mm following the last dye application, mounted for microscopy, and directly visualized.

In brief, two-photon fluorescence lifetime imaging microscopy (FLIM) (Szmacinski and Lakowicz, 1993; Masters *et al*, 1997; Tadrous, 2000) to determine pH was performed by using a Millenia-pumpcd Tsunami titanium:sapphire laser system (Spectra-Physics) as the two-photon excitation source. Excitation of the sample was achieved by coupling the 820 nm output of the laser through the epifluorcscccnce port of a Zeiss Axiovert microscope. The fluorescence was collected using a Hamamatsu (R3996) photomultiplier placed at the bottom port of the microscope. Scanning mirrors and a 40 × infinity corrected oil objective (Zeiss F Fluar, 1.3 NA) were used to image areas of 107 μm^2. Z-slices (1.7 μm per slice) were obtained by adjusting the objective focus with a motorized driver (ASI Multi-Scan 4). Lifetime data were acquired using the frequency-domain method (80 MHz). Fluorescein was used as the reference lifetime standard ($\tau_f = 4.05$ ns, pH 9.5). Data-evaluation and visualization were performed directly with the in-house software SIM-FCS. Fluorescence-intensity images were adjusted to enhance structural features and to visualize dye distribution and penetration. Lifetime-values were converted to pH-values, based on a calibration of BCECF in a series of buffers of different pH.

The resulting pH-maps are displayed on the same color-scale to facilitate comparisons. The pH-value distribution within these images is depicted in the corresponding histograms. For some experiments, these histograms were imported into Origin (Origin Laboratory Corporation, Northampton, MA) to form a reconstruction graph of pH values over depth. Individual images were combined using Adobe Illustrator (Adobe Systems Incorporated, San Jose, CA), but no further image processing was performed. Background fluorescence was measured in samples of unstained tissue, treated otherwise identically.

Conventional surface pH measurements were performed using a flat glass surface electrode (Mettler-Toledo, Giessen, Germany) with a pH meter (Skin pH Meter PH 900; Courage & Khazaka, Cologne, Germany).

Light microscopy

Fresh tissue biopsies were directly immersed in formalin, and stored at 4 °C until paraffin embedding. 5 μm sections were cut, and routinely H&E stained. Images were taken on a Zeiss Axiovert Microscope.

Ultrastructural methods

Freshly obtained biopsies from newborn rat skin (taken from the same animals used for FLIM and light microscopy experiments) were fixed directly in modified Karnovsky's fixative, postfixed with reduced osmium tetroxide (OsO_4), and then embedded in an Epon-epoxy mixture. For visualization of lipid-enriched, lamellar bilayer structures, some samples were postfixed with ruthenium tetroxide ($Ru0_4$). Sections were cut on a Reichcrt Ultracut E microtome, counterstaincd with uranyl acetate and lead citrate, and viewed in a Zeiss 10 CR electron microscope, operated at 60 kV.

Immunohistochemistry

Fresh biopsies from newborn rats, or from fetal rats obtained by C-section, were formaldehyde fixed, paraffin-embedded, and sectioned (5 μm). For immunolabeling of NHE1, a rabbit polyclonal antibody was used (Chemicon Int., Temecula, CA), which was detected via a FITC-labeled, secondary goat anti rabbit antibody (Capped, Organon Teknika Corp., Durham, NC). Sections were counterstained with propidium iodide (Sigma, St. Louis, MO), and pictures were taken on a Leica TCS-SP confocal microscope. Detection of β-GlcCer'ase was performed similarly, employing a polyclonal antibody from rabbit (gift from Drs Ginns and Sidranski, NIH).

Western immunoblotting

Full thickness skin was harvested from newborn rats, and incubated in 10 mM ethylenediaminetetraacetic acid (EDTA) solution for 30 min. The epidermis was subsequently separated by gentle scraping, and membrane fractions (Triton-X100 soluble fraction) prepared. Similarly, membrane fractions were prepared from cultured human keratinocytes, directly immersed in Triton-X100 buffer. The protein contents of individual samples were determined, and gels were loaded with equal amounts per sample and lane. Western immunoblotting was performed using sodium dodecyl sulfate polyacrylamide gel electrophoresis (SDS-PAGE), as described previously (Laemmli, 1970). Following transfer of protein to polyvinylidene difluoride (PVDF) membranes, NHE1 was detected via a monoclonal mouse antibody (Chemicon Int., Temecula, CA). The secondary antibody (peroxidase-conjugated anti mouse; Amersham Pharmacia Biotech Inc., Piscataway, NJ) was followed by final detection with chemiluminescence (ECL-kit, Amersham). For AB/AG competition studies, the primary antibody was preabsorbed with the peptide used for creating the antibody (Alpha Diagnostic, San Antonio, TX). Similarly, β-GlcCer'ase expression was assessed in the same samples, employing the antibody mentioned above.

Equal loading per sample was controlled via individual protein content analysis and Coomassie Brilliant Blue staining of the SDS gels following transfer to PVDF membranes. Additionally, densitometry was performed on the final chemiluminescence images, using the Biorad GS-710 scanner, and Quantity One analysis software. Optical density (OD) values were first adjusted to average background density of the film, and normalization was achieved by reprobing the same PVDF membrane with an anti β-actin antibody (clone AC-74, Sigma, St. Louis, MO). Expression values were normalized within same samples, and averaged values per condition/time point compared by two-tailed *t* test. Finally, a percentage value for the average difference was calculated. Molecular sizes were calculated by a regression analysis based on the prestained color standards routinely used for PAGE.

RESULTS

Neonatal SC displays incomplete lipid processing

We first assessed the structural integrity and maturity of rat skin over the first 5 postnatal days. Light microscopy of fixed, H&E stained sagittal sections revealed a normal-appearing epidermis, although the hyperplasia in our samples was possibly less pronounced as previously reported (Hoath *et al*, 1993). On the first postnatal day (**Fig 1**, *panel A*), the epidermis was completely covered by a tightly apposed pcridermal layer (**Fig 1**, *panel B*). This layer began to separate into discontinuous, surface patches at day 3 (**Fig 1**, *panel C, D*), and was largely absent by day 4 (**Fig 1**, *panel E*).

Electron microscopy also confirmed the presence of a continuous sheet/layer of periderm over the SC on days 1 and 2 (**Fig 2**, *panel A*; cf. **Figure 1**; data for day 2 not shown). By day 3, this layer became less cohesive and adherent to the underlying SC (**Fig 2**, *panel C*). Electron microscopy of ruthenium tetroxide postfixed material also revealed incompletely processed, extracellular lipids in both day 1 and day 2 postnatal SC (**Fig 2**, *panel B*; data for day 2

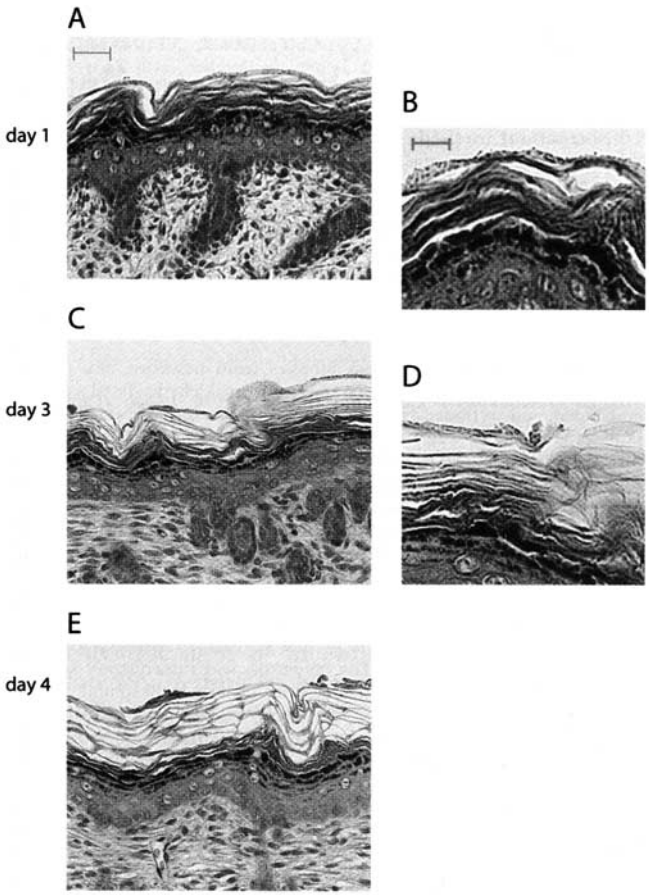

Figure 1. Morphology of neonatal epidermis is normal at birth. Light microscopic images of H&E stained sections, neonatal day 1, 3, and 4. At low magnification (*panels A, C, E*), a normal-appearing epidermis is present. At high magnification, periderm is visible as an intact sheet on day 1 (*panel B, arrows*), begins to recede on day 3 (*panel D*), and is present only in remnants on day 4 (*panel E*). (Scale bar represents 20 μm for A,C,E, and 10 μm for B,D).

not shown). By day 3, however, sections revealed a normal pattern of mature, extracellular lamellar bilayers, indicative of complete lipid processing (**Fig 2**, *panel D*). Similar, mature (processed) lipid also was found in samples from postnatal days 4 and 5 (not shown). Together, these results show that neonatal SC contains barrier competent, mature structures by 3 days after birth.

Surface pH declines to adult levels over one week in the neonatal rat

We next assessed changes in surface pH, using flat electrode measurements, over the first postnatal week in neonatal rats. Newborn rat SC developed an increasingly acidic pH over this period, which achieved adult levels by day 7 (**Fig 3**). After this date, hair growth made surface pH measurements less reliable. Traditional skin surface pH measurements, using flat electrodes, provide reliable information only about surface pH changes, without further vertical or subcellular spatial resolution; ie, specific microdomains such as the corneocytc interstices are not resolved, and the deeper SC is inaccessible without resorting to inherently disruptive stripping methods (van der Molen *et al*, 1997). Therefore, while a decrease in surface pH occurs during the neonatal period, more precise localization of pH/acidification in epidermal/SC microdomains that would allow elucidation of mechanistic issues is lacking.

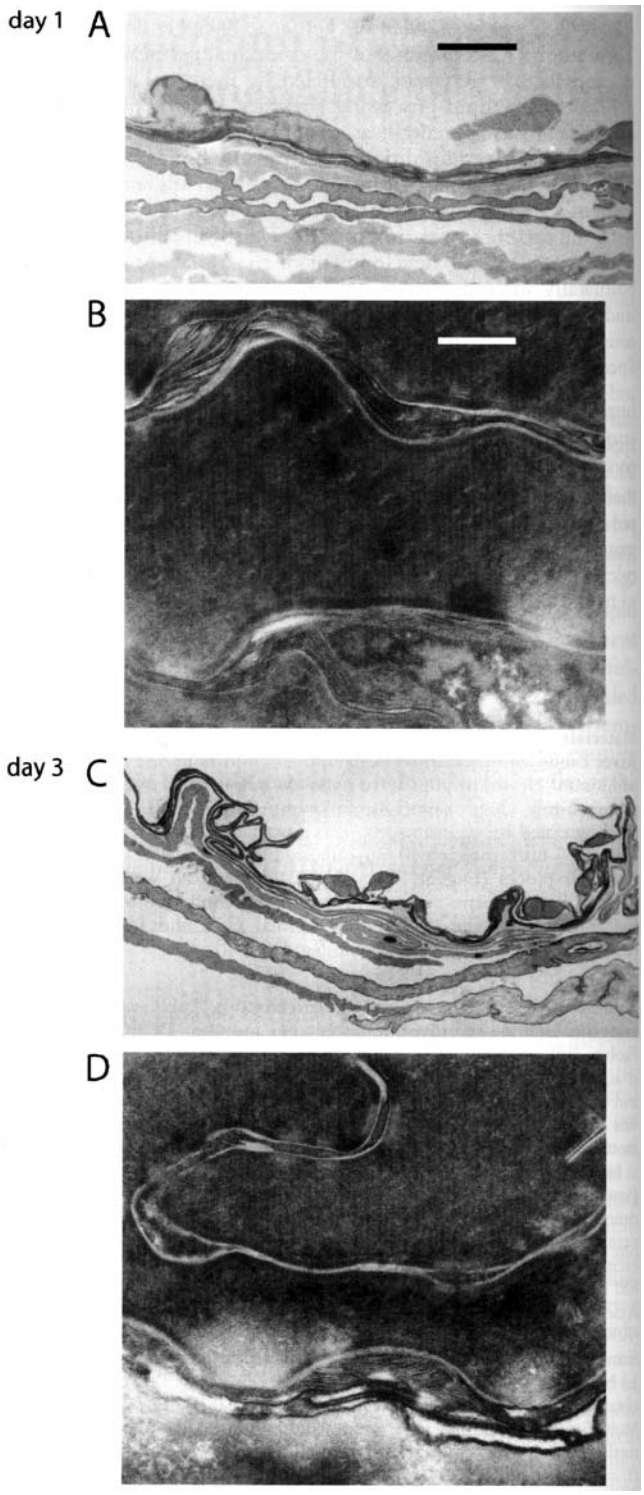

Figure 2. Ultrastructure of neonatal SC normalizes by day 3. Osmium postfixed samples show the periderm as an additional leaflet on the outer aspect of the SC, continuous on day 1 (*panel A*), and partially disrupted on day 3 (*panel C*). Ruthenium postfixed samples of neonatal rat skin reveal areas of incomplete extracellular bilayers on the first postnatal day, visible both at the SC/SG interface and in the superjacent mtercorneo-cytc space (*panel B*). On day 3 post birth mature extracellular bilayers can be observed in intercorneocytc spaces, now condensed to tight lamellar structures, while unprocessed lipids remain at the SC/SG interface (*panel D*), a pattern typically seen in mature, adult SC. (scale bar in *A* and *C* represents 2 μm; in *B* and *D*, 0.25 μm).

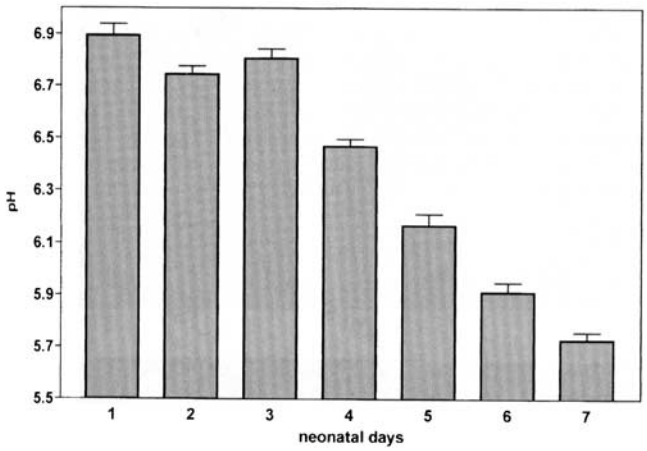

Figure 3. SC surface pH develops over the first postnatal week. Flank skin of neonatal rats was measured using a flat electrode at days 1 through 7 (sec Materials and Methods; values + SEM, $n = 11$–15). A gradual increase in acidity over the first postnatal week is observed.

Acidity begins in membrane domains at the SC/SG interface and spreads outward

Previous studies comparing FLIM with flat electrode measurements showed that FLIM is far more sensitive than flat electrodes, and provides further information about the localized pH microenvironment of adult murine SC (Behne *et al*, 2002; Hanson *et al*, 2002). Therefore, we next assessed changes in pH distribution by FLIM in SC of newborn rats from birth through the fifth postnatal day. During the first postnatal day, only neutral pH values (>pH 6.5) were present throughout the SC, but acidity was detectable in the periderm layer at the skin surface, overlying the SC. This localized apical acidity is best seen in the pH map as the green-dotted pattern of acidic values, colocalizcd to the rounded peridermal structures (**Fig 4**, *panel A, red arrows*). The pH histograms derived from these sections demonstrate neutral values throughout the SC, notably at the SC/SG interface (**Fig 4**, *panel B*), except for localized acidity in the periderm, located above the surface of the SC (**Fig 4**, *panel A*). This pattern did not substantially change during the second postnatal day, indicating the continued presence of a neutral pH throughout the SC (data not shown). By day 3, acidic microdomains were largely, though still incompletely developed at the SC/SG interface (**Fig 4**, *panel D*), best demonstrated in the histograms, which displayed both an acidic (~pH 6) and a neutral (~pH 7) peak both at the surface (**Fig 4**, *panel C* and the SC/SG interface (**Fig 4**, *panel D*). By day 4, the periderm was largely absent, surface sections displayed normal SC structure, and extracellular acidity was present at all levels of the SC (**Fig 4**, *panel E and F, blue arrows*), reflecting the pattern of acidity seen in normal adult mice (Behne *et al*, 2002; Hanson *et al*, 2002). Moreover, the histograms derived from pH maps, first at day 3 and thereafter display a distribution of acidic and neutral pH spikes, which was qualitatively identical to adult murine SC, where a clear colocalization of extracellular domains with acidic pH values is apparent (Behne *et al*, 2002). We did not assess pH distribution in adult rats, because the epidermis becomes very thin and abundant hair follicles make assessment of SC layers by FLIM unreliable. Nevertheless, previous pH electrode measurements on adult rats revealed a pH in the acidic range (Draize, 1942), although somewhat closer to neutral if measured on unshaved skin (Meyer and Neurand, 1991).

To more precisely localize the origin and development of SC acidity, two-dimensional diagrams of pH distribution were constructed. **Figure 5** displays diagrams combining a full scries of histograms from the skin surface to the SG, per postnatal day. The diagrams for days 1–3 showed acidity increasing initially in the periderm (day 1 and 3; **Fig 5**, *panel A and B, asterisks*; day 2 not shown), with values that peaked in this location at day 3. More importantly, a separate increase in acidity became distinguishable at the SC/SG interface on day 3 (**Fig 5**, *panel B*). On the 4th day, the periderm was no longer evident, and a continuously spreading, acidic pH domain that mirrored the adult-pattern ''acid mantle'' was present (**Fig 5**, *panel C*, with little change thereafter (day 5, **Fig 5**, *panel D*). An adult pattern of SC acidity, consisting of both an acidic (~pH 6) and a neutral (~pH 7) peak in the histograms of surface and SC/SG interface, is first evident in rat SC at day 3, and extends uniformly from the SC/SG interface throughout the SC by day 4. Day 5 displays the same pattern as day 4, with a slightly accentuated predominance of the inside-out generation of acidity (**Fig 5**, *panel D*).

Together, these results show that acidity develops in distinct, separate membrane microdomain compartments within the SC. Initially, acidity is limited to within the periderm, and beginning on the third postnatal day, develops inside-out from the SC/SG interface, extending through the entire SC thereafter. These results also show that up to and including day 3, there is a spatial discontinuity between the acidity that develops at the SC/ SG interface and the acidity that is present at the surface, within the periderm. This discontinuity suggests that acidity at the SC/SG interface versus acidity in the periderm stem from separate processes.

Delayed acidification despite full NHE1 expression at birth

In our previous work, we demonstrated the importance of the sodium/hydrogen antiportcr NHE1 for SC acidification, and that this antiporter primarily acidifies the SC/SG interface (Behne *et al*, 2002). Since the FLIM data show that acidification begins at the SC/SG interface, and then radiates outward, we next assessed whether delayed postnatal acidification reflects a parallel delay in the expression of this proton transporter. Because it is not possible to measure NHE1 activity directly *in vivo*, we examined changes in antiporter expression and localization in late fetal and neonatal rat epidermis by Immunohistochemistry and Western irnrnunoblotting. Whereas NHE1 protein was only minimally evident in suprabasal layers at fetal day 17, its amount steadily increased, reaching a maximum expression in all suprabasal layers on fetal day 21, just before birth (term = day 22). Following birth, NHE1 expression continued in the SG localizing to the apical plasma membrane, where it is optimally positioned to extrude protons into the SC/SG interface. Yet, despite progressive localization of this antiporter to outer nucleated layers (**Fig 6**; data corresponding to fetal days 17, 19, 20, and neonatal days 2–4 not shown), overall expression declined slightly postnatally, not only by immunohistochemistry, but also by Western irnrnunoblotting. NHE1 protein levels peaked at day one, but decreased by ~30% by day five following birth ($n = 3$ each, $P = 0.01$; **Fig 7**, *top panel*). Together, these studies indicate that NHE1 is already fully expressed and apically positioned to influence initial acidification at birth. However, the SC/SG interface is not acidified at birth, even with adequate amounts of NHE1 present, suggesting that additional factor(s) trigger initial SC/SG acidification.

Delayed lipid processing despite full β-GlcCer'ase expression at birth

Since the periderm acidity docs not lead to complete lipid processing (**Fig 2**), we conclude that the SC/SG acidity must develop before normal lipid processing can occur (Behne *et al*, 2002). To confirm that increased postnatal lipid processing is due to

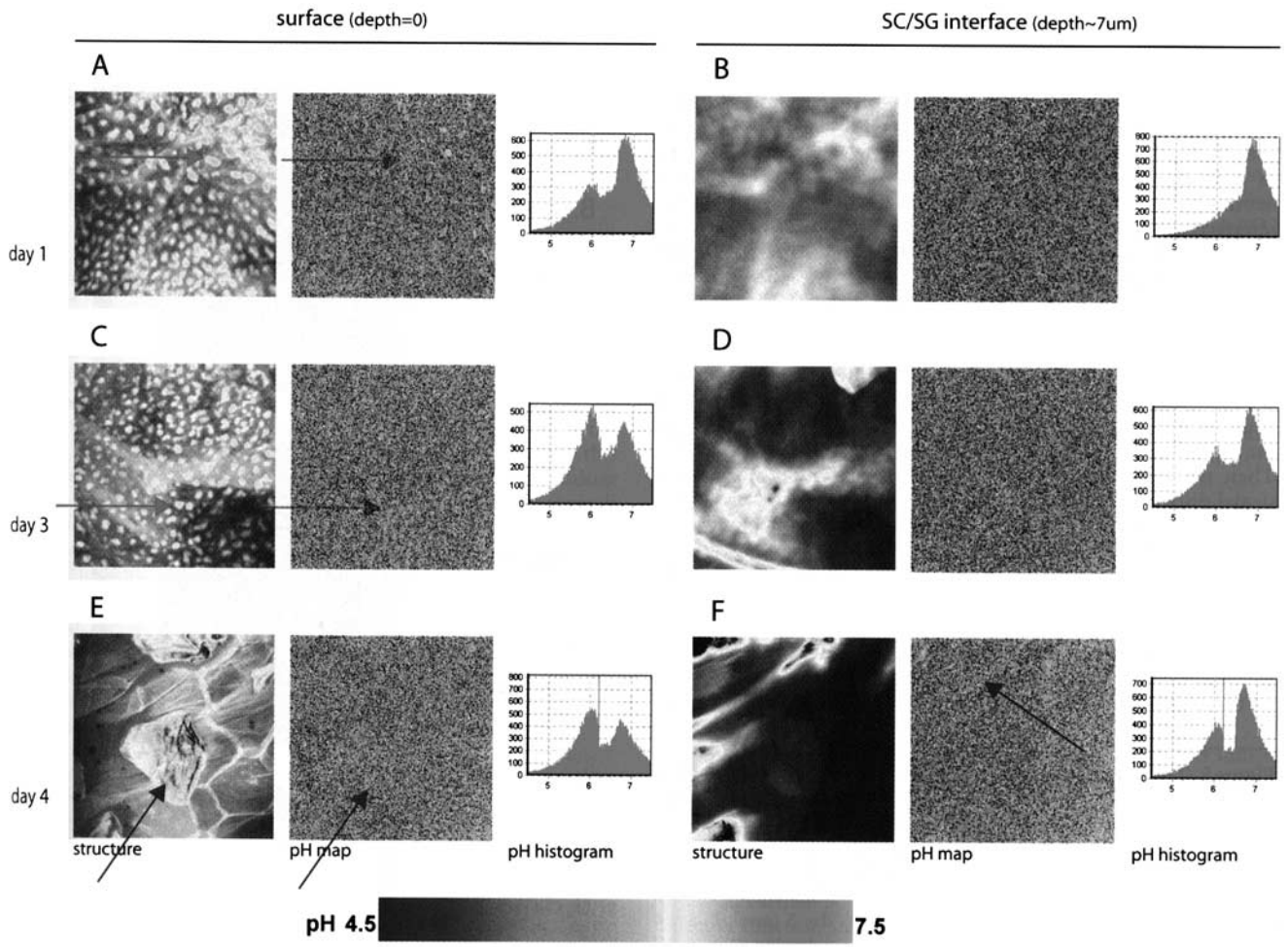

Figure 4. Surface and SC/SG interface pH develops over the first postnatal week. SC pH in neonatal rats on postnatal day 1 (*panels A* and *B*), day 3 (*panels C* and *D*), and day 4 (*panels E* and *F*). The panels show fluorescence intensity images that identify SC structures (grayscale, *left column;* image dimension: 107 μm square), FLIM values converted to pH maps of the same optical section (pseudocolor, *middle column;* color scale of the pH calibration given at the *bottom* of the figure, *blue* representing acidic, and *red* representing neutral domains), and histograms of values for the pH maps (*right column*), both for surface- (or periderm-) levels (*panels A, C, E*) and SC/SG interface-levels (*panels B, D, E*; intermediate levels not shown). Periderm is noted on the surface at day 1 and day 3 (*panels A* and C, *red arrows*), but has receded by day 4 (*panel E*). Microdomains of acidity appear first at the SC/SG interface (day 3, histogram, *panel D*). The extracellular domain (identifiable in the *grayscale images*) is more acidic (*blue arrows*) than the intracellular domain on day 4 (*panels E, F*). Experiments were performed in triplicate, and typical findings are shown.

an increasingly acidic SC pH and not a simple increase in β-GlcCer'asc protein, we assessed β-GlcCcr'ase levels by Western irnrnunoblotting and immunohistochemistry Western irnrnunoblotting for β-GlcCer'ase in newborn epidermis revealed a series of immunorcactive bands, representing β-GlcCer'ase and additional bound saposins (eg, Weiler *et al*, 1995), multimeric forms, and/or the genetic heterogeneity of this enzyme (Sa Miranda *et al*, 1988). All these immunorcactive species displayed a decrease of expression levels between postnatal day 1 and 5, and densitometry on the reported, specific band (Carstea *et al*, 1992) revealed an approximately 85% decrease ($n=3$ each, $P=0.05$; **Fig 7**, *bottom panel*). Immunohistochemistry confirmed that β-GlcCcr'asc levels increase *in utero*, but do not increase between fetal day 21, just prior to birth, and neonatal day 5 (data not shown). Since supra-normal amounts of β-GlcCer'asc enzyme are present at birth, and additional proteolytic cleavage and/or activation is not required, it is the neutral pH of neonatal SC, not differences in β-GlcCer'ase protein that is responsible for incomplete lipid processing between birth and the third postnatal day.

DISCUSSION

Although basal epidermal barrier function in term infants suffices to ensure survival, recent studies suggest that the newborn skin barrier function is not as robust or resilient as that in children or adults. In fact, neonatal skin displays a well-known propensity to develop dermatitis and microbial infections (Berg *et al*, 1994; Rowen *et al*, 1995; Singer *et al*, 1998). Thus, newborn skin must undergo further postnatal developmental adjustments to achieve optimal function in the dry ex-utero environment. We have hypothesized and assessed here whether development of an acidic SC pH results in the final developmental steps of SC maturation. Whereas the transition to an acidic pH is prolonged over several weeks in humans, it is compressed into less than one week in the neonatal rat model used in this study. We found that although the sequence of postnatal pH developmental events could be followed using the conventional surface pH electrode, FLIM technology allows for simultaneous assessment of surface and microdomain pH.

Our recent work with FLIM shows that the acid mantle of mature, adult SC (Hanson *et al*, 2002) consists of an extra-corneo-cyte domain

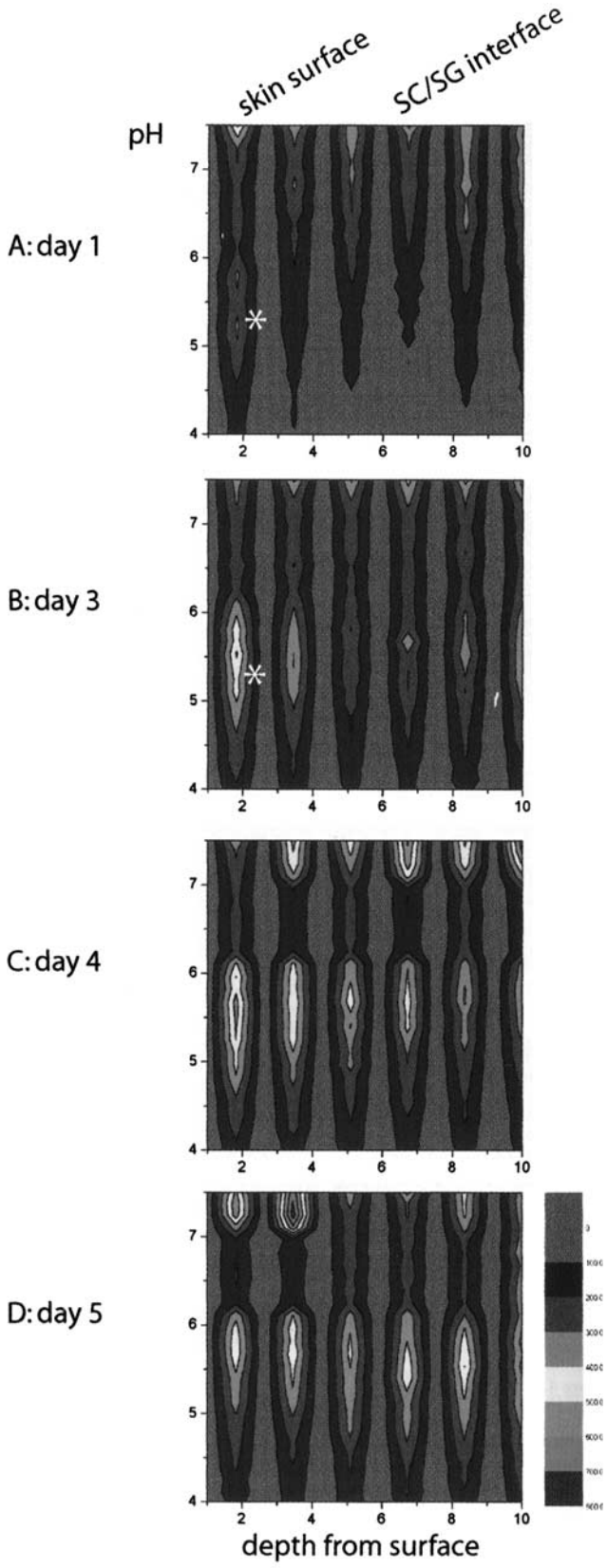

with equally acidic values present at all SC levels, which extends outward from the SC/SG interface. The pH gradient consists of the gradually increasing acidic extracellular domain over the neutral intracorneocyte domains. Our data demonstrated that NHE1 is the mechanism for the sustained acidification at the SC/SG interface level in adult rodent SC (Behne *et al*, 2002). Lipid processing leading to full barrier competence is mostly completed by the region immediately above the SC/SG interface (Fartasch *et al*, 1993; Holleran *et al*, 1993). Thus, initial acidification of extracellular domains in the lower SC correlates with ultrastructural evidence of formation of mature lamellar membranes at these levels. An acidic SC controls lipid processing and epidermal barrier repair through specific pH-dependent lipid hydrolases (β-GlcCer'ase, aSM'ase) that arc essential for SC lipid precursor processing. These hydrolases arc

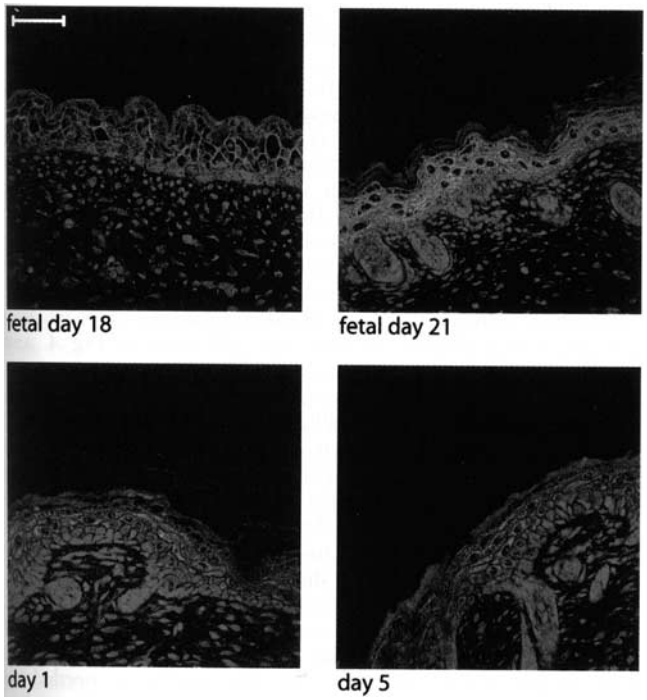

Figure 6. NHE1 localization in rat epidermis over the perinatal period. Note the increasing expression from fetal days 18–21, followed by a slight reduction at neonatal day 1. A subtle decrease in NHE1 abundance is apparent by immunohistochemistry between neonatal days 1 and 5. (scale bar represents 20 μm).

Figure 5. The pH gradient develops between neonatal days 1 and 3. Reconstruction of pH histograms derived from image series of neonatal days 1–5. Displayed are the peak intensities of the measured pH range, *versus* the tissue depth, from the skin surface to the SC/SG interface. The *y-axis* displays the same pH scale as the histograms in **Fig. 4**, the x-axis represents the distance from the skin surface, and pH intensity/counts arc color-coded as in the scale included in panel D. Day 1 (*panels A*), day 3 (*panels B*), day 4 (*panels C*), and day 5 (*panels D*). The histograms show development of SC acidity (intensity peak between pH 4.5 and pH 6) from day 1 to day 4 beginning at the SC/SG interface. Surface acidity (*asterixes*) seen in day 1 (*panels A*) and day 3 (*panels B*) is derived from the periderm. All diagrams in comparison show acidity increasing initially at the surface, which peaks at day 4, and in parallel, but separately increasing acidity at the SC/SG interface, which by day 4 forms a continuously spreading extracellular acidic pH domain (*panels C*), while pH distribution inside-out dominates thereafter (*panels D*).

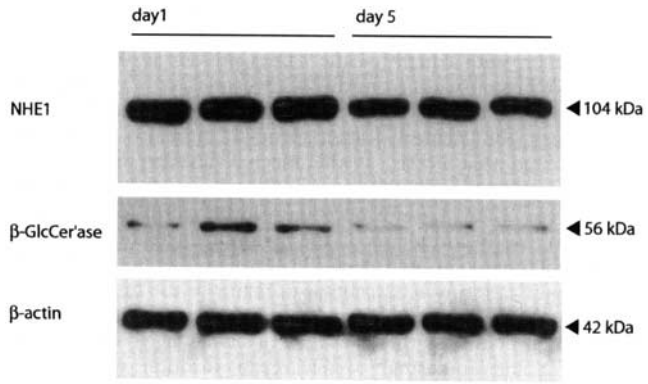

Figure 7. Expression levels for NHE1 and β-GlcCer'ase decrease following birth. Western Immunoblot for NHE1 and β-GlcCer'ase from newborn (day 1) and 5-day-old epidermis. Three individual animals per time point were evaluated, and expression levels were normalized to β-actin (*bottom panel*). NHE1 (*top panel*) exhibits approximately 30% reduction of expression. The calculated size of the single immunoreactive band was 104 kDa. In initial experiments, we identified NHE1 protein in human foreskin keratinocytes (CHK) on Western Immunoblots. Controls including preimmune serum, and antibody/antigen competition studies demonstrated the specificity of the immunodetection for NHE1 (not shown). The calculated, approximate mass of the single, specific 111 kDa band correlated well with the reported size for human NHE1 (McSwine *et al*, 1994); a slight size difference is presumably attributable to phosphorylation (Goss *et al*, 1996). The approximate, calculated size from newborn rat epidermis, employing the same monoclonal anti-NHEl antibody as for human cells, is 104 kDa. Although reported sizes for other rat tissues may differ (Orlowski *et al*, 1992), we here also find a single immuno-reactive band, most likely identical to the fully glycosylated form of this protein (Goss *et al*, 1996). β-GlcCer'ase (*middle panel*) exhibits approximately 85% reduction of expression, parallel to NHE1. This smallest size immunoreactive band on our blots (i.e., 56 kDa) matches the reported mouse isoform (Carstea *et al*, 1992) (additional immunoreactive bands with calculated sizes of 94 and 78 kDa not shown).

less active when SC is exposed to a neutral pH (Mauro *et al*, 1998), consistent with their known acidic pH optima (Jensen *et al*, 1999; Takagi *et al*, 1999; Schmuth *et al* 2000). Clearly, such correlations within localized domains are not possible with standard flat electrodes, which measure only surface pH. Moreover, sequential tape-stripping of SC layers introduces artifacts through its inherently disruptive nature, and the inability to remove specific, homogeneous layers of the SC (van der Molen *et al*, 1997). The novel FLIM technique recently developed for epidermal use by our group (Hanson *et al*, 2002) reveals heretofore undetectable, spatio-temporal details about the development of the epidermal pH gradient, and provides a unique opportunity to gain insight from pH localization as correlated with SC structural/functional alterations. Since the SC acid mantle regulates not only epidermal barrier homeostasis (Thune *et al*, 1988; Berg *et al*, 1994; Mauro *et al*, 1998), but also key SC functions such as desquamation (Ohman and Vahlquist, 1998), and antimicrobial capacity (Aly *et al*, 1978; Korting *et al*, 1990), FLIM results also will provide insights into the role of pH in regulating these and other SC functions.

Potentially SC Acidifying Mechanisms

Although a number of mechanisms have been proposed for the generation of SC acidity, this remains an active area of investigation. We previously have shown that H^+ generated by NHE1 located in the SG are an important source of SC acidity (Behne *et al*, 2002). In addition, primarily catabolic processes within the SC generate acidic end-products that can affect SC pH. Two prominent examples for these intrinsic processes are: (1) the breakdown *o* proteins such as filaggrin to produce urocanic acid (Krien and Kermici, 2000); and (2) the hydrolysis of lipids, such as PL, to yield FFA (Fluhr *et al*, 2001). The latter may occur cither intrinsically through specific phospholipascs (Schadow *et al*, 2001), or extrinsically as byproducts of microbial metabolism (Korting *et al*, 1987). As additional acidic material may be deposited onto the SC surface from skin appendages (e.g., lactic acid and lactate from sweat (Patterson *et al*, 2000), and sebum-derived free fatty acids (Lieckfeldt *et al*, 1995), these latter pathways may be characterized as extrinsic to the intcrfollicular epidermis, as they begin acidification at the SC surface.

Acidification of newborn SC could result from the gradual accumulation of protons from any of these sources. Nevertheless, the extrinsic sources lactic acid/sweat (Patterson *et al*, 2000) and free fatty acids/sebum (Lieckfeldt *et al*, 1995) appear to be of minor importance to newborn animals, since neither sweat- nor sebaceous glands will be fully developed or fully active in animals that have not yet developed fur. Microbial colonization also appears to contribute only a minor amount to normal SC acidity, both because conditions such as humidity that enhance bacterial growth decrease in postnatal SC (Aly *et al*, 1978; Hartmann, 1983; Scott and Harding, 1986; Hoath *et al*, 1992), and because bacterial colonization does not change in the immediate neonatal period, between the first and fifth postnatal days ('J.W. Fluhr, M.J. Behnc, B. E. Brown, D. G. Moskowitz, C. Scldcn,T. M. Mauro, P. M. Elias & K. R. Feingold (2002). Stratum Corneum Acidification in Neonatal Skin: I. Secretory Phospholipase A2 and the NHE1 Antiporter Acidify Neonatal Rat Stratum Corneum *J Invest Dermatol* submitted.). Together, these findings exclude bacterial colonization as a major pathway in generating acidity in the newborn.

Our FLIM data demonstrates that the acidity that correlates with effective lipid processing develops initially in the extracellular compartment of the lower SC. This localization further excludes the above-mentioned extrinsic pathways, as these would acidify the SC in an outside-in manner. Further, the localization of acidity in the lower SC docs not appear compatible with the intrinsic process of urocanic acid generation (Krien and Kermici, 2000), which should be localized to, or at least originate from, the intracellular compartment of the corneocytc, which in all our FLIM experiments appears as a domain of neutral pH (compare e.g., pH maps in **Fig 4**, and (Behne *et al*, 2002; Hanson *et al*, 2002)).

There is evidence that another instrinsic SC acidification pathway, FFA generated from PL by secretory phospholipasc A2 (Fluhr *et al*, 2001), contributes to SC acidification. Since the SC sPLA2 isoform(s) that could generate FFA have not yet been completely identified and characterized, the specificity and significance of pharmacological inhibitors that were employed to assess the role of sPLA2 remain to be resolved (e.g., Singer *et al*, 2002). Further, based on the pKa of the predominant SC FFA (Lieckfeldt *et al*, 1995; Kanicky *et al*, 2000), it is not yet evident how a pH as acidic as present in the SC could be produced by this pathway alone. The PL-to-FFA mechanism is also complicated by the prospect that acidity is needed to incorporate FFA into the lipid bilaycr system, rather than acidity being supplied through FFA (Bouwstra *et al*, 1998; Lieckfeldt *et al*, 1995; Bouwstra *et al*, 2000). Together, these data suggest that the extent to which PL-derived FFA participate in neonatal SC acidification remains unresolved.

Our data suggest that an intrinsic process that localizes to the lower SC or SC/SG interface is the primary agent that acidifies the newborn SC. The NHE1 has been clearly identified as the Na^+/H^+ antiporter isoform present in kcratinocytcs and epidermis

(Sarangarajan *et al*, 2001; Behne *et al*, 2002) and has been shown to acidify the SC in adult mice (Behne *et al*, 2002). The data shown here demonstrate that in newborn rat epidermis NHE1 also is expressed and localized to provide protons directly to the SC, thus acidifying SC in newborn epidermis, as previously shown for adult SC.

Role of the periderm in neonatal acidification

In this study, the periderm was prominent over the first two postnatal days. *In utero*, the periderm as a transitory fetal layer interfaces between developing epidermis and amniotic fluid, serving a multitude of purposes and functions (Hoyes, 1968; Holbrook and Odland, 1975; Weiss and Zelickson, 1975a; Weiss and Zelickson, 1975b; Weiss and Zelickson, 1975c), including transport/exchange with amniotic fluid. To this purpose, it expresses tight junctions much like simple epithclia (Morita *et al*, 2002). In later stages of fetal development, its function may be reduced to a mechanical protection of the growing fetus (Kartasova *et al*, 1996). At a stage where amniotic fluid is generated mainly from the fetus's renal secretions, the skin becomes impermeable (Parmley and Seeds, 1970), waterproofing the fetus (Wickett *et al*, 1993), and thus protecting it from unwanted amniotic contents. Periderm possibly contributes to post–natal barrier function, albeit incompletely, as newborn skin exhibits a functional epidermal permeability barrier despite the delayed formation of extracellular lamellar membranes. Therefore the additional layer of periderm may have a passive role in the developing epidermal barrier, while it allows for a prolonged in-utero/ex-utero transition.

Our present FLIM results show that the intact periderm itself is acidic, while the underlying SC remains neutral until postnatal day 3. As such, the periderm may provide an initial, minimal environment for enzymatic lipid processing activity to neonatal epidermis in an outward-in fashion, which is not sufficient to assure formation of mature lamellar lipid bilayers throughout the SC. Further studies to elucidate the presence and function of specific periderm dissolution products in neonatal SC acidification clearly are required to elucidate the role of periderm in the final maturation of the epidermal barrier during the in-utero/ex-utero transition.

In parallel to periderm dissolution, the SC appears to develop a transitory hyperplasia, which peaks at day 3 (Hoath *et al*, 1993). This hyperplasia may explain the decrease in expression of the specific proteins we examined, β-ClcCer'ase and NHE1. While neither the expression levels of NHE1, nor the levels required for optimal/minimal barrier function, were known prior to this study, the changes in its expression appear relatively minor. In contrast, the precipitous drop in expression of β-GlcCer'ase was surprising. For adult epidermis enzyme levels were reported to exceed barrier requirements several-fold (Holleran *et al*, 1992, 1993). The reduction of enzyme expression in newborn rats may therefore reflect the transitory accumulation of enzyme in SC, which is gradually replaced following birth. Alternatively, supernormal levels *in utero* and directly at birth could also indicate a compensation for the ''incorrect,'' suboptimal pH conditions. Nevertheless, the magnitude of change indicates that further studies arc required to elucidate this development.

In summary, the experiments described here demonstrate that newborn epidermis is fully equipped with both a mechanism to acidify the SC, via NHE1 activity, and a mechanism to process lipids in its extracellular compartment, via β-GlcCer'ase activity. We demonstrate that postnatal SC acidification takes place analogous to SC acidification in the adult, where this inside-out process begins at the SC/SG interface, with acidification proceeding outward to the SC surface with time. We speculate that air exposure after birth, and resultant desiccation of the SC, furnishes the activating trigger for intrinsic acidification processes, including activation of NHE1, to provide the initial step in establishing SC acidity at the SC/SG interface. This SC acidity is required for full lipid processing, and provides a mechanism that allows establishment of an optimum epidermal permeability barrier both in neonatal and adult epidermis.

ACKNOWLEDGMENTS

This work was supported by VA Merit Review MAU3 (TM), NIH HD29706 (KF), and the San Francisco Veteran's Affairs Hospital.

REFERENCES

Aly R, Shirley C, Cunico B, Maibach HI (1978) Effect of prolonged occlusion on the microbial flora, pH, carbon dioxide and transcpidermal water loss on human skin. *J Invest Dermatol* 71:378–81

Aszterbaum M, Menon GK, Fcingold KR, Williams ML (1992) Ontogeny of the epidermal barrier to water loss in the rat: Correlation of function with stratum corneum structure and lipid content. *Pcdiatr Res* 31:308–17

Behne MJ, Meyer JW, Hanson KM *et al* (2002) NHE1 regulates the stratum corneum permeability barrier homeostasis. Microenvironmcnt acidification assessed with fluorescence lifetime imaging. *J Biol Chem* 277:47399–406

Behrendt H, Green M (1958) Skin pH pattern in the newborn infant. *AMA Journal of Diseases of Children* 95:35–41

Berg RW, Milligan MC, Sarbaugh FC (1994) Association of skin wetness and pH with diaper dermatitis. *Pediatr Dermatol* 11:18–20

Bouwstra JA, Gooris GS, Dubbclaar FE, Ponec M (2000) Phase behaviour of skin barrier model membranes at pH 7.4. *Cell Mol Biol* 46:979–92

Bouwstra JA, Gooris GS, Dubbclaar FE, Wccrheim AM, Ponec M (1998) pH, cholesterol sulfate, and fatty acids affect the stratum corneum lipid organization. *J Invest Dermatol Symp Proc* 3:69–74

Carstea ED, Murray GJ, O'Neill RR (1992) Molecular and functional characterization of the murine glucocercbrosidase gene. *Biochem Biophys Res Comnmn* 184:1477–83

Cunico RL, Maibach III, Khan H, Bloom E (1977) Skin barrier properties in the newborn. Transcpidermal water loss and carbon dioxide emission rates. *Biol Neonate* 32:177–82

Draize JH (1942) The determination of the pH of the skin of man and common laboratory animals. *J Invest Dermatol* 5:77–85

Fartasch M, Bassukas ID, Diepgen TL (1993) Structural relationship between epidermal lipid lamellae, lamellar bodies and desmosomes in human epidermis: An ultra-structural study. *Br J Dermatol* 128:1–9

Fluhr JW, Kao J, Jam M, Aim SK, Feingold KR, Elias PM (2001) Generation of free fatty acids from phospholipids regulates stratum corneum acidification and integrity. *J Invest Dermatol* 117:44–51

Fox C, Nelson D, Wareham J (1998) The timing of skin acidification in very low birth weight infants. *J Perinatol* 18:272–5

Goss G, Orlowski J, Grinstein S (1996) Coimmunoprccipitation of a 24-kDa protein with NHE1, the ubiquitous isoform of the Na^+/H^+ exchanger. *Am J Physiol* 270:C1493–502

Hanley K, Jiang Y, Holleran WM, Elias PM, Williams ML, Feingold KR (1997) Glucosyl-ccramidc metabolism is regulated during normal and hormonally stimulated epidermal barrier development in the rat. *J Lipid Res* 38:576–84

Hanson KM, Behne MJ, Barry NP, Mauro TM, Gratton E, Clegg RM (2002) Two-photon fluorescence lifetime imaging of the skin stratum corneum pH gradient. *BiophysJ* 83:1682–90

Harpin VA, Rutter N (1983) Barrier properties of the newborn infant's skin. *J Pediatr* 102:419–25

Hartmann AA (1983) Effect of occlusion on resident flora, skin-moisture and skin-pH. *Arch Dermatol Res* 275:251–4

Hoath SB, Pickens WL, Tanaka R, Ross R (1992) Ontogeny of integumental calcium in relation to surface area and skin water content in the perinatal rat. *J Appl Physiol* 73:458–64

Hoath SB, Tanaka R, Boyce ST (1993) Rate of stratum corneum formation in the perinatal rat. *Invest Dermatol* 100:400–6

Holbrook KA, Odland GF (1975) The fine structure of developing human epidermis: Light, scanning, and transmission electron microscopy of the periderm. *J Invest Dermatol* 65:16–38

Holleran WM, Takagi Y, Imokawa G, Jackson S, Lec JM, Elias PM (1992) beta-Glucocereb-rosidase activity in murine epidermis. Characterization and localization in relation to differentiation. *J Lipid Res* 33:1201–9

Hollcran WM, Takagi Y, Menon GK, Lcglcr G, Fcingold KR, Elias PM (1993) Processing of epidermal glucosylccramides is required for optimal mammalian cutaneous permeability barrier function. *J Clin Invest* 91:1656–64

Hoycs AD (1968) Electron microscopy of the surface layer (periderm) of human foetal skm. *J Anat* 103:321–36

Jensen JM, Schutzc S, Fori M, Kronke M, Proksch E (1999) Roles for tumor necrosis factor receptor p55 and sphingomyelinase in repairing the cutaneous permeability barrier. *J Clin Invest* 104:1761–70

Kanicky JR, Poniatowski AF, Mchta NR, Shah DO (2000) Coopcrativity among molecules at interfaces in relation to various technological processes: Effect of chain length on the pKa of fatty acid salt solutions. *Langmuir* 16:172–7

Kartasova T, Darwiche N, Kohno Y *et al* (1996) Sequence and expression patterns of mouse SPR1: Correlation of expression with epithelial function. *J Invest Dermatol* 106:294–304

Korting HC, Hubner K, Greincr K, Hamm G, Braun-Falco O (1990) Differences in the skin surface pH and bacterial microflora due to the long-term application of synthetic detergent preparations of pH 5.5 and pFl 7.0. Results of a crossover trial in healthy volunteers. *Acta Derm Venercol* 70:429–31

Korting HC, Kobcr M, Mueller M, Braun-Falco O (1987) Influence of repeated washings with soap and synthetic detergents on pH and resident flora of the skin of forehead and forearm. Results of a cross-over trial in health probationers. *Acta Derm Venereol* 67:41–7

Krien PM, Kermici M (2000) Evidence for the existence of a self-regulated enzymatic process within the human stratum corneum -An unexpected role for urocanic acid. *J Invest Dermatol* 115:414–20

Laemmli UK (1970) Cleavage of structural proteins during the assembly of the head of bacteriophage T4. *Nature* 227:680–5

Lieckfeldt R, Villalain J, Gomez-Fernandez JC, Lee G (1995) Apparent pKa of the fatty acids within ordered mixtures of model human stratum corneum lipids. *Pharm Res* 12:1614–7

Masters BR, So PT, Gratton E (1997) Multiphoton excitation fluorescence microscopy and spectroscopy of in vivo human skin. *BiophysJ* 72: 2405–12

Mauro T, Hollcran WM, Grayson S *et al* (1998) Barrier recovery is impeded at neutral pH, independent of ionic effects: Implications for extracellular lipid processing. *Arch Dermatol Res* 290:215–22

McSwine RL, Babnigg G, Musch MW, Chang EB, Villcreal ML (1994) Expression and phosphorylation of NIIE1 in wild-type and transformed human and rodent fibroblasts. *J Cellular Physiol* 161:351–7

Meyer W, Neurand K (1991) Comparison of skin pH in domesticated and laboratory mammals. *Arch Dermatol Res* 283:16–8

Sa Miranda MC, Aerts JM, Pinto RA, Magalhacs JA, Barranger JA, Tager JM, Schram AW (1988) Heterogeneity in human acid beta-glucosidase revealed by cellulose- acetate electrophoresis. *Biochim Biophys Acta* 965:163–8

van der Molen RG, van Spies F, 't Noordcndc JM, Boclsma E, Mommaas AM, Koerten HK (1997) Tape stripping of human stratum corneum yields cell layers that originate from various depths because of furrows in the skin. *Arch Dermatol Res* 289:514–8

Morita K, Furuse M, Yoshida Y, Itoh M, Sasaki H, Tsukita S, Miyachi Y (2002) Molecular architecture of tight junctions of periderm differs from that of the maculae occludentes of epidermis. *J Invest Dermatol* 118:1073–9

Ohman H, Vahlquist A (1998) The pH gradient over the stratum corneum differs in X-linked recessive and autosomal dominant ichthyosis: a clue to the molecular origin of the ''acid skin mantle''? *J Invest Dermatol* 111:674–7

Orlowski J, Kandasamy RA, Shull GE (1992) Molecular cloning of putative members of the sodium, proton exchanger gene family: cDNA cloning, deduced amino acid sequence, and mRNA tissue expression of the rat sodium, proton exchanger NHE-1 and two structurally related proteins. *J Biol Chem* 267:9331–9

Parmley TH, Seeds AE (1970) Fetal skin permeability to isotopic water (THO) in early pregnancy. *Am J Obstet Gynecol* 108:128–31

Patterson MJ, Galloway SD, Nimmo MA (2000) Variations in regional sweat composition in normal human males. *Exp Physiol* 85:869–75

Pickens WL, Warner RR, Boissy YL, Boissy RE, Hoath SB (2000) Characterization of ver-nix caseosa: Water content, morphology, and elemental analysis. *J Invest Dermatol* 115:875–81

Rowen JL, Atkins JT, Levy ML, Baer SC, Baker CJ (1995) Invasive fungal dermatitis in the greater than or equal to 1000-gram neonate. *Pediatrics* 95:682–7

Sarangarajan R, Shumaker H, Soleimani M, Le Poole C, Boissy RE (2001) Molecular and functional characterization of sodium — hydrogen exchanger in skin as well as cultured keratinocytes and melanocytes. *Biochim Biophys Acta* 1511:181–92

Schadow A, Scholz-Pcdretti K, Lambeau G, Gelb MH, Furstenbergcr G, Pfeilschifter J, Kaszkin M (2001) Characterization of group X phospholipasc A (2) as the major enzyme secreted by human keratinocytes and its regulation by the phorbol ester TPA. *J Invest Dermatol* 116:31–9

Schmuth M, Man MQ, Weber F *et al* (2000) Permeability barrier disorder in Niemann-Pick disease: Sphingomyelin- ceramide processing required for normal barrier homeostasis. *J Invest Dermatol* 115:459–66

Scott IR, Harding CR (1986) Filaggrin breakdown to water binding compounds during development of the rat stratum corneum is controlled by the water activity of the environment. *Dev Biol* 115:84–92

Seidenari S, Giusti G (1995) Objective assessment of the skin of children affected by atopic dermatitis: A study of pFl, capacitance andTEWL in eczematous and clinically uninvolvcd skin. *Acta Dermato-Venereologica* 75:429–33

Singer AG, Ghomashchi F, Le Calvcz C *et al* (2002) Intcrfacial Kinetic and Binding Properties of the Complete Set of Human and Mouse Groups I, II, V, X, and XII Secreted Phospholipases A2. *J Biol Chem* 277:48535–49

Singer S, Singer D, Ruechcl R, Mergcryan H, Schmidt U, Harms K (1998) Outbreak of systemic aspergillosis in a neonatal intensive care unit. *Mycoses* 41:223–7

Szmacinski H, Lakowicz JR (1993) Optical measurements of pH using fluorescence lift-times and phase- modulation fluorometry. *Anal Chem* 65:1668–74

Taddei A (1935) Ricerche, mediante indicatori, sulla relazionc attuale della cute nel neona- to. *Riv Ital Ginec* 18:496

Tadrous PJ (2000) Methods for imaging the structure and function of living tissues and cells: 2. Fluorescence lifetime imaging. *J Pathol* 191:229–234

Takagi Y, Kriehuber E, Imokawa G, Elias PM, Holleran WM (1999) Beta-glucocerebrosi-dase activity in mammalian stratum corneum. *J Lipid Res* 40:861–9

Thune P, Nilscn T, Hanstad IK, Gustavsen T, Lovig Dahl H (1988) The water barrier function of the skin in relation to the water content of stratum corneum, pH and skin lipids. The effect of alkaline soap and syndet on dry skin in elderly, non-atopic patients. *Acta Derm Venereol* 68:277–83

Visscher MO, Chatterjee R, Munson KA, Pickens WL, Hoath SB (2000) Changes in diapered and nondiapered infant skin over the first month of life. *Pediatr DemMld* 17:45–51

Visscher M, Hoath SB, Conroy E, Wickett RR (2001) Effect of semipermeable membrane on skin barrier repair following tape stripping. *Arch Dermatol Res* 293:491–9

Weiler S, Kishimoto Y, O'Brien JS, Barrangcr JA, Tomich JM (1995) Identification of the binding and activating sites of the sphingolipid activator protein, saposin C, with glucocerebrosidasc. *Protein Sci* 4:756–64

Weiss LW, Zelickson AS (1975a) Embryology of the epidermis: Ultrastructural aspects. I. Formation and early development in the mouse with mammalian comparisons. *Acta Derm Venereol* 55:161–8

Weiss LW, Zelickson AS (1975b) Embryology of the epidermis: Ultrastructural aspects. II. Period of differentiation in the mouse with mammalian comparisons. *Acta Derm Venereol* 55:321–9

Weiss LW, Zelickson AS (1975c) Embryology of the epidermis: Ultrastructural aspects. III, Maturation and primary appearance of dendritic cells in the mouse with mammalian comparisons. *Acta Derm Venereol* 55:431–42

Wickett RR, Mutschelknaus JL, Hoath SB (1993) Ontogeny of water sorption-desorption in the perinatal rat. *J Invest Dermatol* 100:407–11

Wilhelm KP, Maibach HI (1990) Factors predisposing to cutaneous irritation. *Dermatol Gin* 8:17–22